

# On the effects of rotation on acoustic stellar pulsations: validity domains of perturbative methods and close frequency pairs

K. D. Burke,<sup>1\*</sup> D. R. Reese<sup>1,2</sup> and M. J. Thompson<sup>1,3</sup>

<sup>1</sup>Department of Applied Mathematics, University of Sheffield, Hicks Building, Hounsfield Road, Sheffield S3 7RH

<sup>2</sup>Observatoire de Paris, LESIA, CNRS UMR 8109, 92195 Meudon, France

<sup>3</sup>High Altitude Observatory, National Center for Atmospheric Research, Boulder, CO 80307, USA

Accepted 2011 January 29. Received 2011 January 24; in original form 2010 November 21

## ABSTRACT

Pulsation frequencies of acoustic modes are calculated for realistic rotating stellar models using both a perturbative and a two-dimensional approach. A comparison between the two yields validity domains which are similar to those previously obtained in Reese et al. for polytropic models. One can also construct validity domains based on polynomial fits to the frequencies from the two-dimensional approach, and these also turn out to be similar, thus further confirming the agreement between the perturbative and the two-dimensional approaches at low rotation rates. Furthermore, as was previously shown in Espinosa et al., adjacent frequencies in multiplets come close together, thus forming pairs. This phenomenon, exclusive to two-dimensional calculations, is shown to be an unlikely explanation of the close frequency pairs observed in  $\delta$  Scuti stars. A systematic search for all close frequency pairs in the calculated spectrum is also carried out. The number of close frequency pairs is shown to agree with what is expected based on a Poisson distribution, but does not match the number or distribution of close pairs in stars such as FG Vir. Furthermore, a lack of close frequency pairs appears at low rotation rates, where frequency multiplets do not overlap.  $\delta$  Scuti stars currently reported as having close frequency pairs do not fall in this interval.

**Key words:** stars: oscillations – stars: rotation.

## 1 INTRODUCTION

The new space missions, *CoRoT* and *Kepler*, are substantially increasing the accuracy with which stellar pulsations are observed. A look at *CoRoT*'s and *Kepler*'s first asteroseismic results shows the progress that has been made in the photometric detection of solar-like oscillations, as well as the substantial increase in the number of detected modes in earlier type stars such as  $\delta$  Scuti stars (Michel et al. 2008; Kjeldsen et al. 2010). The high duty cycle and the long observational runs (up to 5 months for *CoRoT* and several years for *Kepler*) are key factors in this dramatic improvement. As a result, there is a drive on the theoretical side to achieve accurate computations of pulsation frequencies in stellar models. Although a fair amount of success has been achieved in slowly rotating stars, much work is still needed before being able to accurately model pulsation modes in rapidly rotating stars. This is because at rapid rotation rates, the centrifugal force causes stellar deformation thereby transforming what used to be a one-dimensional eigenvalue problem into one that is two dimensional. This is all the more problematic as many stars rotate rapidly.

In order to address the effects of rotation, two different methods have been developed. The first is the perturbative method which starts from a non-rotating star and then includes various corrections which model the effects of rotation. These corrections are generally expressed as a power series in terms of the rotation rate which is assumed to be a small parameter. Previous works include Saio (1981), Gough & Thompson (1990) and Dziembowski & Goode (1992) for the second order, and Soufi, Goupil & Dziembowski (1998) and Karami et al. (2005) for the third order. The advantage of this method is that it is computationally less expensive and mode classification is more straightforward, thereby allowing an efficient study of an entire spectrum of pulsation modes for a given model. However, this method is only valid for slow rotation rates. The other approach consists in solving directly the two-dimensional eigenvalue system. Previous works which focus on p modes include Clement (1981), Yoshida & Eriguchi (2001), Espinosa, Pérez Hernández & Roca Cortés (2004), Lignières, Rieutord & Reese (2006) and Lovekin & Deupree (2008). Although computationally more expensive, this method can handle pulsation modes at any rotation rate. A natural question is at what rotation rates does it become necessary to use a two-dimensional approach rather than a perturbative approach.

A number of previous works have focused on answering the above question in the case of acoustic modes. In Reese, Lignières

\*E-mail: k.burke@sheffield.ac.uk

**Table 1.** Model parameters.

$M$ ( $M_{\odot}$ )	Age (Gyr)	$\Omega/\Omega_K$	$\Omega$ (rad s $^{-1}$ )	$R$ ( $R_{\odot}$ )	$L$ ( $L_{\odot}$ )	$T_{\text{eff}}$ (K)	$h_{\Omega}(R)$
1.00	0.00	0.0	0.00	0.89	0.69	5573.9	0.00
1.00	0.00	$2.0 \times 10^{-5}$	$1.50 \times 10^{-8}$	0.89	0.69	5573.9	$1.40 \times 10^{-10}$
1.00	0.00	$2.0 \times 10^{-4}$	$1.50 \times 10^{-7}$	0.89	0.69	5573.9	$1.40 \times 10^{-8}$
1.00	0.00	$2.0 \times 10^{-3}$	$1.50 \times 10^{-6}$	0.89	0.69	5573.9	$1.40 \times 10^{-6}$
1.00	0.00	$2.0 \times 10^{-2}$	$1.50 \times 10^{-5}$	0.89	0.69	5573.5	$1.40 \times 10^{-4}$
1.00	0.00	$2.0 \times 10^{-1}$	$1.49 \times 10^{-4}$	0.89	0.67	5534.6	$1.44 \times 10^{-2}$
2.00	0.00	0.0	0.00	1.60	17.30	9307.87	0.00
2.00	0.00	$2.0 \times 10^{-5}$	$8.76 \times 10^{-9}$	1.60	17.30	9307.87	$1.35 \times 10^{-10}$
2.00	0.00	$2.0 \times 10^{-4}$	$8.76 \times 10^{-8}$	1.60	17.30	9307.87	$1.35 \times 10^{-8}$
2.00	0.00	$2.0 \times 10^{-3}$	$8.76 \times 10^{-7}$	1.60	17.30	9307.86	$1.35 \times 10^{-6}$
2.00	0.00	$2.0 \times 10^{-2}$	$8.76 \times 10^{-6}$	1.60	17.30	9307.18	$1.35 \times 10^{-4}$
2.00	0.00	$2.0 \times 10^{-1}$	$8.61 \times 10^{-5}$	1.62	17.20	9240.81	$1.39 \times 10^{-2}$

& Rieutord (2006), validity domains were established for third-order perturbative methods. The underlying stellar models were polytropic and the perturbative calculations were, in fact, polynomial fits to the non-perturbative<sup>1</sup> frequencies. Later on, Lovekin & Deupree (2008) did comparisons using more realistic models. Once more, the perturbative calculations were polynomial fits to the non-perturbative frequencies. Given the larger error bars on the calculations, perturbative calculations were considered to be valid up to higher rotation rates. Other works include Ouazzani et al. (2009) where non-perturbative frequencies were compared with frequencies resulting, this time, from a perturbative analysis rather than a polynomial fit. Furthermore, the effects of avoided crossings were included in the perturbative calculations and shown to improve the agreement with two-dimensional calculations. Finally, Suárez et al. (2010) investigated the effects of perturbative and non-perturbative frequencies of polytropic models on echelle diagrams and various frequency separations. They showed that including avoided crossings in perturbative analysis becomes necessary for correctly predicting the behaviour of the small frequency separation, even at relatively low rotation rates. None the less, a systematic study of the validity of perturbative methods for realistic models is still lacking. Given the accuracy of the new pulsation data coming from the *CoRoT* and *Kepler* missions, such a study is needed in order to correctly interpret these data. Therefore, in this work, we will compare two-dimensional calculations with frequencies resulting from a second-order perturbative analysis and establish validity domains similar to those in Reese et al. (2006). These calculations will be carried out for acoustic modes, using realistic stellar models rather than polytropic ones. Furthermore, we will discuss some of the qualitative differences between the two types of calculations.

The next section deals with the stellar models. This is then followed by a description of the perturbative and two-dimensional pulsation calculations. Section 4 compares the results from the two approaches and Section 5 deals with close frequency pairs, both within multiplets and for an entire spectrum. Finally, Section 6 concludes this paper with a discussion.

## 2 MODELS

Stellar models were created using the Aarhus stellar evolution code, ASTEC (Christensen-Dalsgaard 2008a). The OPAL 1995 opacity

<sup>1</sup> The term ‘non-perturbative frequencies’ in this context means frequencies based on a two-dimensional calculation, rather than frequencies in which the effects of rotation have been removed.

tables (Iglesias & Rogers 1996) were used in conjunction with the Kurucz low-temperature adjustments (Kurucz 1991) and the Eggleton, Faulkner and Flannery equation of state (Eggleton, Faulkner & Flannery 1973). Evolution begins at zero-age main sequence (ZAMS) and continues to a user-specified age. The initial mass  $M$ , angular velocity  $\Omega$  and hydrogen and heavy element abundances  $X$  and  $Z$ , respectively, are also set by the user. The models calculated here are 1 and 2  $M_{\odot}$  ZAMS models with solar elemental abundances and rotation rates ranging from  $\Omega/\Omega_K = 0$  to 0.25, where  $\Omega_K = \sqrt{GM/R^3}$  and  $R$  is the stellar radius. A selection of the models calculated is given in Table 1.

The effects of rotation were then included to second order in rotational velocity,  $\Omega$ . In particular, the stellar structure is no longer spherically symmetric but oblate due to the centrifugal force. We therefore perform a transformation of the coordinate system  $(r, \theta, \phi) \rightarrow (x, \theta, \phi)$ , from a system of shells of constant radius,  $r$ , to shells of constant pressure, chosen such that  $x = R$  maps the surface of the star which can now be treated as a surface in hydrostatic equilibrium. The new radial coordinate  $x$  takes the form

$$x = [1 + h_{\Omega}(r)P_2(\cos\theta)]r, \quad (1)$$

where  $h_{\Omega}$  is the transformation coefficient and  $P_2(\cos\theta) = \frac{3\cos^2\theta - 1}{2}$ , the  $\ell = 2$  Legendre polynomial. This can be inverted to give, to order  $\Omega^2$ ,

$$r = [1 - h_{\Omega}(x)P_2(\cos\theta)]x. \quad (2)$$

We define a function  $u = h_{\Omega}x$  such that  $u$  satisfies the following second-order differential equation:

$$\mathcal{H}u = \mathcal{G}(x), \quad (3)$$

where

$$\mathcal{H} \equiv \frac{d^2}{dx^2} + \left( \frac{8\pi x^2 \rho_0}{Mq_0} - \frac{2}{x} \right) \frac{d}{dx} - \frac{4}{x^2}, \quad (4)$$

$$\mathcal{G}(x) = \frac{4\pi x^4 \rho_0}{GM^2 q_0^2} \left[ f_{r2} - \frac{d}{dx}(x f_{\theta 2}) \right] + \frac{6x f_{\theta 2}}{GMq_0} - \frac{1}{GMq_0} \frac{d}{dx} \left[ x^2 \frac{d}{dx}(x f_{\theta 2}) \right], \quad (5)$$

and  $f_{r0} = -\frac{2}{3}\Omega^2 x$ ,  $f_{r2} = \frac{2}{3}\Omega^2 x$ ,  $f_{\theta 2} = \frac{1}{3}\Omega^2 x$  and  $q_0 = m/M$  is the fractional mass interior to a radius  $x$ . Boundary conditions for this

system are

$u$  regular as  $x \rightarrow 0$

$$u' + \frac{u}{x} = \frac{x^2}{GM} \left[ x \frac{d}{dx} (f_{\theta 2}) + 4f_{\theta 2} \right] \quad \text{at } x = R.$$

The surface boundary condition is found by matching the gravitational potential  $\Phi_0$  on to the vacuum potential for  $x > R$ .

This change in coordinates leads to a change in all variables with a radial dependence such that e.g.  $\rho_0(x) = \rho_0(r) + \rho_\Omega(r)P_2(\cos\theta)$ , where the subscript ‘0’ represents the equilibrium quantity, with similar expressions for  $p_0(x)$  and  $c_0(x)$ .

### 3 PULSATION MODE CALCULATIONS

#### 3.1 Perturbative analysis

In order to calculate perturbative frequencies, we follow closely the method of Gough & Thompson (1990). The perturbation equation, to order  $\Omega^2$ , can be written as

$$\mathcal{L}\xi + \rho_0\omega^2\xi = \omega.\mathcal{M}\xi + \mathcal{N}\xi, \quad (6)$$

where

$$\mathcal{L}\xi = -\nabla \cdot [(p_0 - \rho_0 c_0^2) \nabla \cdot \xi - \xi \cdot \nabla p_0] + p_0 \nabla \cdot (\nabla \cdot \xi) - \xi \cdot \nabla (\ln \rho_0) \nabla p_0,$$

$$\mathcal{M}\xi = -2i\rho_0 \mathbf{v} \cdot \nabla \xi,$$

$$\mathcal{N}\xi = \rho_0 [-\xi \cdot \nabla (\mathbf{v} \cdot \nabla \mathbf{v}) + (\mathbf{v} \cdot \nabla)^2 \xi]. \quad (7)$$

Here  $p_0$ ,  $\rho_0$  and  $c_0$  are the equilibrium pressure, density and sound speed, respectively;  $\omega$  is the angular pulsation frequency and  $\mathbf{v}_0$  is the velocity field resulting from rotation.  $\xi$  is the Lagrangian displacement and is defined such that

$$\xi_{nlm} = \left[ \xi(x) Y_\ell^m(\theta, \phi), \eta(x) \frac{\partial Y_\ell^m(\theta, \phi)}{\partial \theta}, \frac{\eta(x)}{\sin \theta} \frac{\partial Y_\ell^m(\theta, \phi)}{\partial \phi} \right], \quad (8)$$

where  $\xi$  and  $\eta$  are the radial and horizontal amplitude functions, respectively,  $\eta$  is the radial order and  $Y_\ell^m$  the spherical harmonic of degree  $\ell$  and azimuthal order  $m$ . We choose to normalize  $Y_\ell^m$  such that

$$\int_0^{2\pi} \int_0^\pi |Y_\ell^m(\theta, \phi)|^2 \sin \theta d\theta d\phi = 1, \quad (9)$$

and we normalize  $\xi(x)$  such that  $\xi(R) = 1$ .

The structural changes of the equilibrium model resulting from rotation cause perturbations to the eigenfunction  $\xi$  and to the function  $\mathcal{L}\xi$ , denoted, respectively, by  $\xi_1$  and  $\mathcal{L}_\Omega \xi$ . For further details, we refer the reader to Gough & Thompson (1990). These perturbation quantities are substituted into equation (6), and we linearize the resulting expression to second order in rotational velocity  $\Omega$ . This leads to the following expression for the oscillation frequency, valid to second order in  $\Omega$ :

$$\begin{aligned} \omega_{nlm} = & \omega_0 + \omega_{\Omega 1} + (2I\omega_0)^{-1} \langle \xi_0^* \cdot (\mathcal{N}_0 - \mathcal{L}_\Omega - \rho_\Omega P_2 \omega_0^2) \xi_0 \rangle \\ & - \omega_{\Omega 1}^2 (2\omega_0)^{-1} - \omega_{\Omega 1} I^{-1} \langle \rho_0 \xi_0^* \cdot \xi_1 \rangle \\ & + (2I)^{-1} \langle \xi_0^* \cdot \mathcal{M}_0 \xi_1 \rangle \\ & + \omega_{\Omega 1} (2I\omega_0)^{-1} \langle \xi_0^* \cdot \mathcal{M}_0 \xi_0 \rangle, \end{aligned} \quad (10)$$

where  $\langle \dots \rangle = \int_0^{2\pi} \int_0^\pi \int_0^R \dots x^2 \sin \theta dx d\theta d\phi$  is, to first order, the volume integral over the interior of the star.  $\omega_0$  is the unperturbed oscillation frequency,

$$I = \int_0^R \rho_0 x^2 [\xi^2 + \ell(\ell+1)\eta^2] dx, \quad (11)$$

and  $\omega_{\Omega 1}$  contains the terms to first order in  $\Omega$  and can be expressed as

$$\omega_{\Omega 1} = \frac{m}{I} \int_0^R \Omega \rho_0 x^2 [(\xi - \eta)^2 + (\ell(\ell+1) - 2)\eta^2] dx. \quad (12)$$

The ADIPLS adiabatic pulsation package (Christensen-Dalsgaard 2008b) was then modified to include second-order rotational effects and subsequently used to calculate perturbative frequencies.

#### 3.2 Two-dimensional calculations

In order to carry out the two-dimensional pulsation calculations, we used the same approach as in Reese et al. (2009). The pulsation equations are expressed in terms of a new coordinate system which follows the shape of the star, then projected on to the spherical harmonic basis and finally solved using the pulsation code Two-dimensional Oscillation Program (TOP; Reese et al. 2009).

The new coordinate system can be represented by  $(\zeta, \theta, \phi)$ , where  $\zeta$  is the radial coordinate,  $\theta$  is the colatitude and  $\phi$  is the longitude. The relationship between  $\zeta$  and  $r$ , the distance from the origin, is given by the following two equations:

$$r(\zeta, \theta) = (1 - \epsilon)\zeta + \frac{5\zeta^3 - 3\zeta^5}{2} [R_s^*(\theta) - 1 + \epsilon], \quad (13)$$

$$\begin{aligned} r(\zeta, \theta) = & 2\epsilon + (1 - \epsilon)\zeta \\ & + (2\zeta^3 - 9\zeta^2 + 12\zeta - 4) [R_s^*(\theta) - 1 - \epsilon], \end{aligned} \quad (14)$$

where  $\epsilon = 1 - \frac{R_{\text{pol}}^*}{R}$ ,  $R_s^*(\theta) = \frac{R^*}{R} - P_2(\cos \theta) \frac{R^* h_\Omega(R^*)}{R}$ ,  $R_{\text{pol}}^*$  is the polar radius at the last grid point and  $R^*$  is the radial coordinate at the last grid point. The first equation applies to the first domain, i.e. for  $\zeta \in [0, 1]$ , which corresponds to the star. It must be noted that contours of constant  $x$  and  $\zeta$  values do not in general coincide, except at the last grid point where  $x = R^*$  and  $\zeta = 1$ , because only the former corresponds to isobars. As a result, the model must be interpolated on to this new grid. The second equation applies to the second domain, i.e. for  $\zeta \in [1, 2]$ , which lies outside the star and in which only the perturbation to the gravitational potential is used. This coordinate system ensures that the standard regularity conditions can be used in the centre since it behaves like the spherical coordinate system in the centre, and it allows the use of simple boundary conditions both on the stellar surface for the Lagrangian displacement and pressure fluctuations and on the outer boundary of the second domain for the perturbation to the gravitational potential.

The pulsation equations are expressed in terms of the Lagrangian displacement,  $\xi$ :

$$0 = \rho + \nabla \cdot (\rho_0 \xi), \quad (15)$$

$$\begin{aligned} 0 = & [-\omega + m\Omega]^2 \rho_0 \xi - 2i[-\omega + m\Omega] \rho_0 \Omega \times \xi \\ & - \nabla p + \rho \mathbf{g}_{\text{eff}} - \rho_0 \nabla \Psi, \end{aligned} \quad (16)$$

$$0 = p + \xi \cdot \nabla p_0 - c_0^2 (\rho + \xi \cdot \nabla \rho_0), \quad (17)$$

$$0 = \Delta \Psi - 4\pi G \rho, \quad (18)$$

where  $\rho$ ,  $p$  and  $\Psi$  are the density, pressure and gravitational potential fluctuations, respectively. This is the same set of equations as what is given in the appendix of Reese et al. (2009) except that

there is no gradient of the rotation rate, since the rotation profile is uniform, and each occurrence of  $\omega$  has been replaced by  $-\omega$ , so as to ensure that prograde modes correspond to positive values of  $m$ , the azimuthal order. Furthermore, in order to increase the accuracy of the calculations, the effective gravity has been calculated from the gradient of the total potential rather than from the gradient of the pressure divided by the density. For explicit expressions in terms of the spheroidal coordinate system, we refer the reader to Reese et al. (2009).

Calculating pulsation modes in models based on the *ASTEC* code (Christensen-Dalsgaard 2008a) is similar to calculating modes in models based on the self-consistent field method (MacGregor et al. 2007), although there are some noteworthy differences. *ASTEC* models include atmospheres which means that the associated radial grids become very dense near the surface. As a result, care must be taken when expressing the radial differential operator in an algebraic form. For instance, using the fourth-order finite difference implemented in Reese et al. (2009) leads to numerically unstable behaviour. This has been replaced with a more stable version of fourth-order finite differences in which the differential equations are solved on carefully chosen intermediate grid points.

#### 4 VALIDITY DOMAINS FOR PERTURBATIVE CALCULATIONS

Before establishing validity domains for second-order perturbative methods, it is important to compare the two methods for non-rotating (or nearly non-rotating) stars. Differences arise from the different formulations of the pulsation equations and should be correctly characterized before proceeding to establish validity domains. Fig. 1 shows the differences between  $m = 0$  modes calculated with the two methods. Although this error is small, it is larger than the error bar from a *CoRoT* long run and should therefore be taken into account when constructing validity domains.

Fig. 2 shows a comparison between the two methods for three different error bars. The first two correspond to a long and short *CoRoT* run and the third corresponds to 2.3 d of observation. The radial orders of the modes are  $n = 1-10$ , the harmonic degrees  $\ell = 0-3$  and the azimuthal orders  $m = -\ell$  to  $\ell$ . Frequency multiplets calculated using perturbative theory were shifted using the differ-

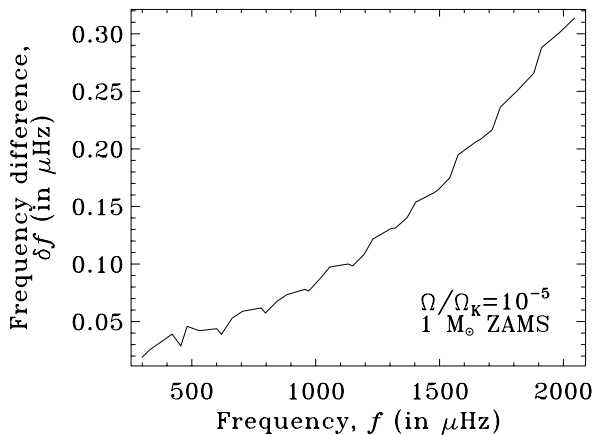


**Figure 1.** A comparison of  $m = 0$  modes for a  $1 M_{\odot}$  model rotating at  $\Omega = 10^{-5} \Omega_K$ . The radial orders are  $n = 1, 10$  and the harmonic degrees  $\ell = 0, 3$ . These differences are larger than  $0.08 \mu\text{Hz}$ , the error bar on a *CoRoT* long run, and must therefore be taken into account when constructing validity domains.

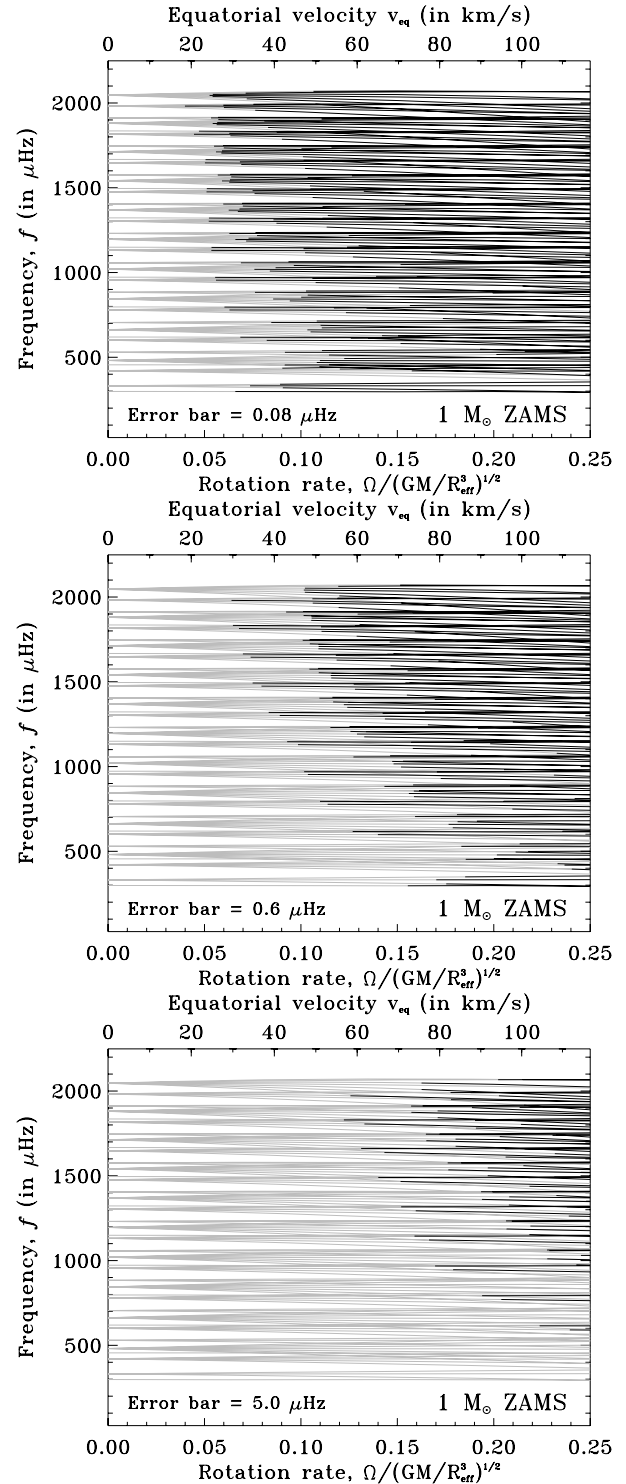


**Figure 2.** Validity domains for second-order perturbative frequencies of  $1 M_{\odot}$  ZAMS models for three different error bars, the first two corresponding to *CoRoT* error bars. These figures are analogous to fig. 4 of Reese et al. (2006), which were established for an  $N = 3$  polytropic model.

ences which are plotted in Fig. 1. This leads to somewhat larger and more realistic validity domains, especially for the smallest error bar. Based on these validity domains, non-perturbative effects will start to play an important role beyond  $v_{\text{eq}} = 30 \text{ km s}^{-1}$  for a long run, and  $v_{\text{eq}} = 50 \text{ km s}^{-1}$  for a short run, in a  $1 M_{\odot}$  star. However, given

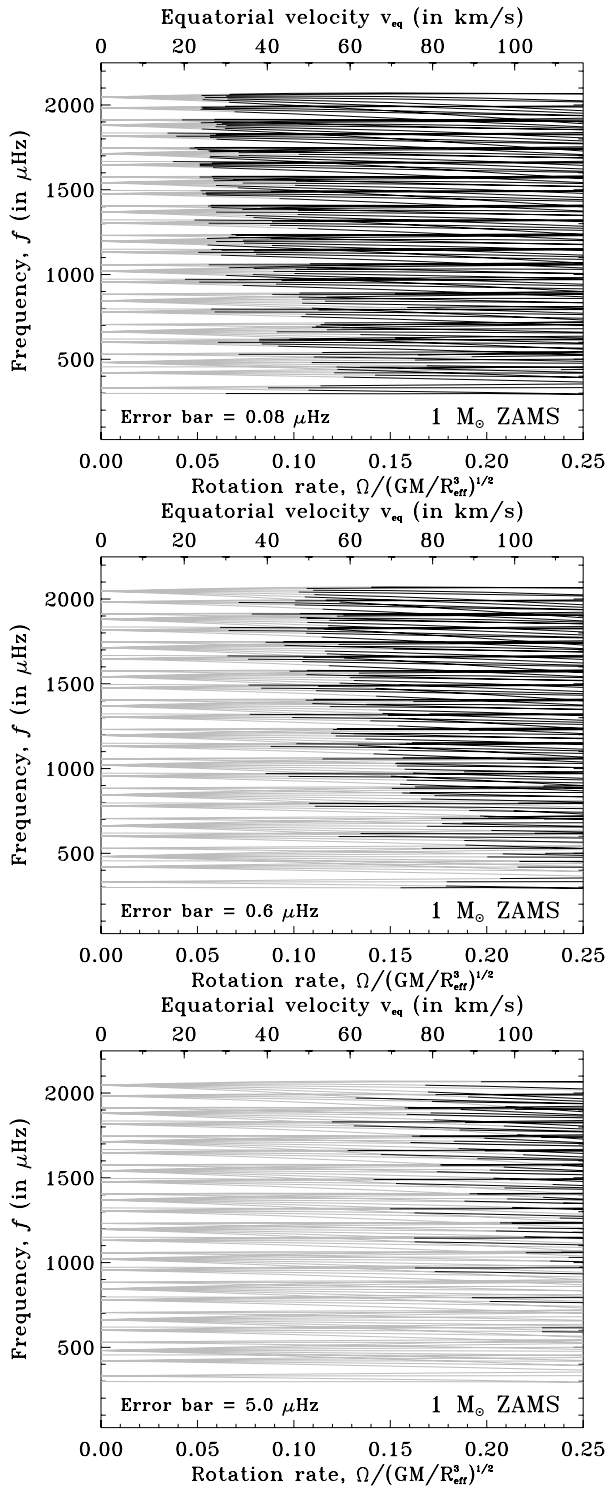


**Figure 3.** Same as Fig. 2 except that the perturbative frequencies have been replaced with second-order polynomial fits to the non-perturbative frequencies.

that solar-like pulsators tend to oscillate with radial orders between 15 and 25, these limits are expected to be lower, as based on the trends which can be seen in Fig. 2.

If the perturbative frequencies are replaced with polynomial fits to the non-perturbative frequencies, similar validity domains are obtained, as can be seen in Fig. 3. This comparison shows that there is

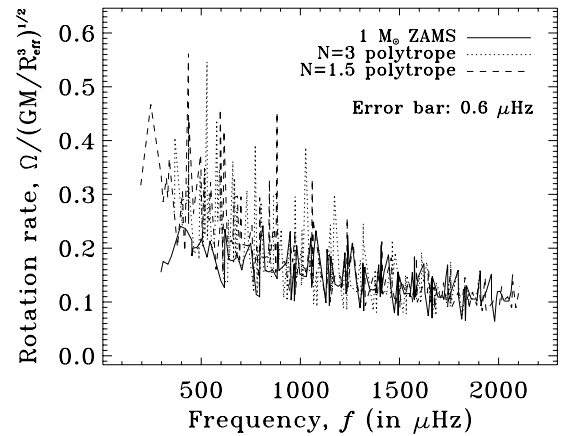


**Figure 4.** Comparison between the validity domains for two polytropic models and the  $1 M_{\odot}$  ZAMS model, for the  $0.6\text{-}\mu\text{Hz}$  error bar. The threshold separating the regions where perturbative methods are valid and not valid is plotted so as to allow the superposition of the different domains.

a good agreement between the polynomial coefficients and the coefficients deduced from perturbative theory, thus providing a further check that both the perturbative and two-dimensional approaches agree at low rotation rates.

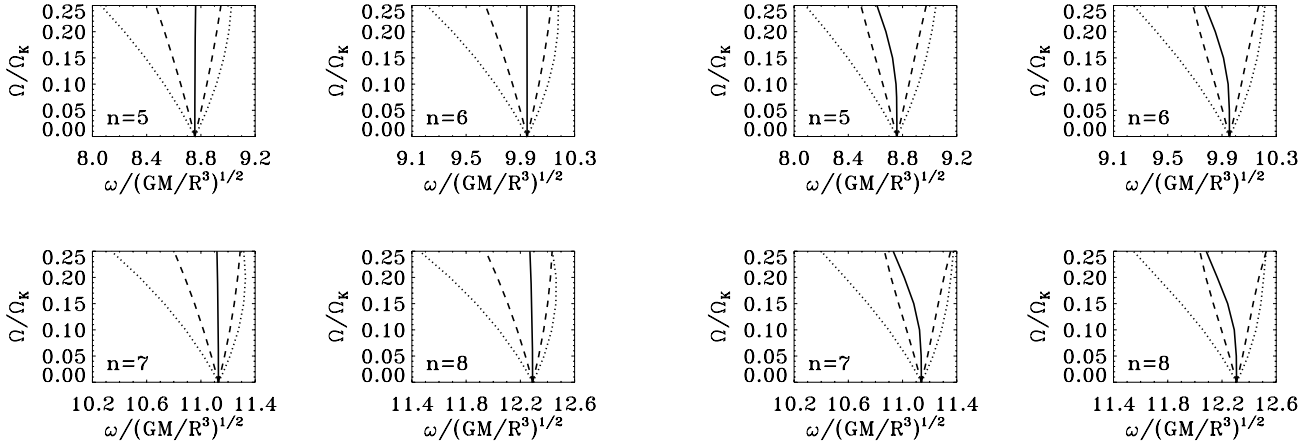
It is then interesting to compare these validity domains with those obtained from polytropic models. Fig. 4 shows such a comparison. It includes the validity domain for  $N = 3$  and  $1.5$  polytropic models and compares them with that of the  $1 M_{\odot}$  ZAMS model using the  $0.6\text{-}\mu\text{Hz}$  error bar. The polytropic models are scaled so as to have the same mass and approximately the same radii<sup>2</sup> as the  $1 M_{\odot}$  ZAMS model. In order to superimpose the different validity domains, we have simply plotted the threshold between the region where the perturbative approach is valid and the region where a two-dimensional calculation becomes necessary. As can be seen from the figure, the validity domains are quite similar. At high frequencies, they follow the same tendency as a function of frequency and have a similar spread around the mean value. At low frequencies, the threshold for the  $1 M_{\odot}$  model seems to be, on average, lower than that of the polytropic models. This effect is, however, likely to be an artefact due to the cut-off at  $\Omega = 0.25 \Omega_K$  for the  $1 M_{\odot}$  frequency calculations (see Fig. 2).

## 5 CLOSE FREQUENCY PAIRS

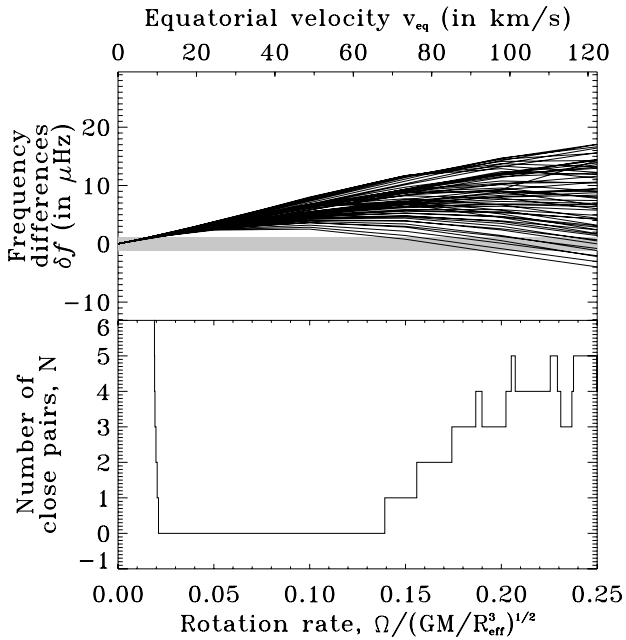
In Espinosa et al. (2004), it was pointed out that adjacent frequencies within a multiplet tend to pair up and come close together, except for the most retrograde mode (i.e.  $m = -\ell$  sectoral mode). It was then suggested that this phenomenon could explain the close frequency pairs observed in Breger & Bischof (2002) (see also Breger & Pamyatnykh 2006a,b). A similar pairing up of modes also occurs for the frequencies in Reese et al. (2006) as well as the non-perturbative frequencies presented here. In what follows, we will consider  $2 M_{\odot}$  ZAMS models, as this is more representative of  $\delta$  Scuti stars. The second half of Table 1 gives the characteristics for a selection of these models.

Fig. 5 shows four sets of  $\ell = 2$  multiplets calculated using both perturbative and two-dimensional calculations. As can be seen in

<sup>2</sup> The polar and equatorial radii were made to satisfy  $\frac{R_{\text{pol}} + R_{\text{eq}}}{2} = 0.89 R_{\odot}$ , which is approximately true of the  $1 M_{\odot}$  ZAMS model.



**Figure 5.** Four  $\ell = 2$  multiplets calculated using perturbative (left) and two-dimensional (right) calculations in  $2M_{\odot}$  models. Frequencies only pair up in the two-dimensional calculations. In the perturbative case, the spacings decrease uniformly when going from the most retrograde to the most prograde mode.



**Figure 6.** Upper panel: frequency differences between adjacent modes in the  $\ell = 1$ – $3$  frequency multiplets of  $2M_{\odot}$  models, as a function of the rotation rate. The frequency span of the spectrum is approximately 250–1060  $\mu\text{Hz}$ . The grey band in the middle corresponds to differences which are less than  $0.1 \text{ c d}^{-1}$ . Lower panel: number of frequency differences below  $0.1 \text{ c d}^{-1}$  as a function of the rotation rate. This number is generally quite low except for slow rotation rates, where the average spacing between frequencies in a multiplet is comparable to  $0.1 \text{ c d}^{-1}$ .

the figures, only the two-dimensional calculations lead to this behaviour. The perturbative calculations produce, instead, spacings which decrease uniformly when going from the most retrograde to the most prograde mode. However, the effects of avoided crossings have not been included in the perturbative calculations, so it remains to be seen whether including this effect can also produce a pairing up of adjacent frequencies.

It is then interesting to investigate whether this effect could explain the close frequency pairs observed in Breger & Pamyatnykh (2006b). In Fig. 6, we compare the frequency differences of mode pairs to a frequency separation of  $0.1 \text{ c d}^{-1}$  (i.e.  $1.1574 \mu\text{Hz}$ ), a typical threshold for observed frequency pairs. As can be seen from

the upper panel, these differences remain larger on average than  $0.1 \text{ c d}^{-1}$ . The lower panel shows the number of sufficiently close frequencies as a function of the rotation rate. As can be seen, this number is not very large for any given rotation rate, except when the rotation rate is around or below  $0.1 \text{ c d}^{-1}$ . However, 18 close frequency pairs were observed in FG Vir (Breger & Pamyatnykh 2006a), and its equatorial velocity is estimated to be  $66 \pm 16 \text{ km s}^{-1}$ , as based on the modelling of line profile variations (Zima et al. 2006). As a result, the pairing up of adjacent modes in frequency multiplets does not seem to account for close frequency pairs in  $\delta$  Scuti stars.

Of course, it is always possible to look at all of the frequency differences for a given spectrum. This approach has been used by Lenz, Pamyatnykh & Breger (2008) to study three  $\delta$  Scuti stars, including FG Vir. Here, we will push the analysis slightly further by looking at how the number of close frequency pairs depends on the rotation rate. Fig. 7 shows the number of close frequency pairs

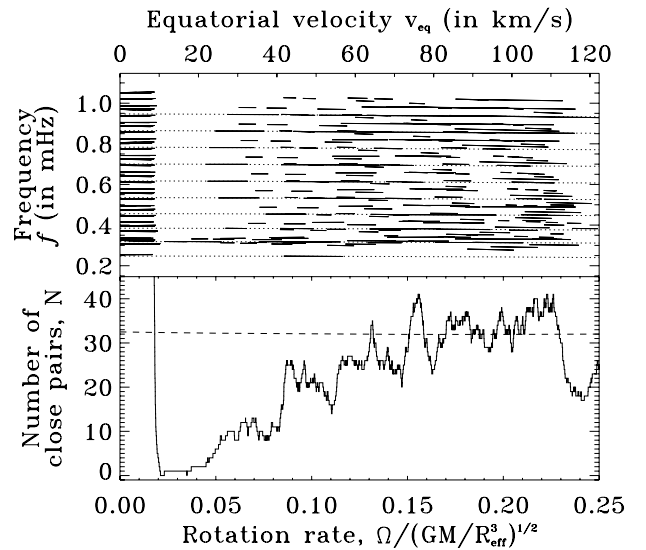


**Figure 7.** Upper panel: close frequency pairs in  $2M_{\odot}$  models as a function of the rotation rate for the frequency spectrum ( $n = 1$ – $10$ ,  $\ell = 0$ – $3$ ,  $m = -\ell$  to  $\ell$ ). The horizontal dotted lines show the location of radial modes. Lower panel: number of close frequency pairs as a function of the rotation rate. The dashed line shows the number of close frequency pairs that is expected for a Poisson distribution.

as a function of the rotation rate as well as where they occur. The dashed line in the lower panel gives the expected number of pairs,  $N_{\text{exp.}}$ , as based on a Poisson distribution:

$$N_{\text{exp.}} = (N_{\text{mode}} - 1) \left[ 1 - \exp\left(-\frac{(N_{\text{mode}} - 1) \delta f}{\Delta f}\right) \right], \quad (19)$$

where  $N_{\text{mode}}$  is the number of modes in the spectrum,  $\Delta f$  the frequency span of the spectrum and  $\delta f$  the target frequency separation (i.e.  $0.1 \text{ c d}^{-1}$ ). At a sufficient rotation rate, the average number of close frequency pairs matches  $N_{\text{exp.}}$ , indicating that the spectrum is behaving like a Poisson distribution. As was pointed out by Lignières & Georgeot (2008, 2009), the frequency spectrum of rapidly rotating stars is subdivided into classes of regular modes, such as these low degree modes and chaotic modes, the frequencies of which follow Poisson and Wigner distributions, respectively, provided there are no selection effects.

The number of close frequency pairs is much higher than in the previous case and higher than the number of pairs observed in FG Vir. However, Fig. 7 is based on 160 frequencies, whereas there are 67 independent frequencies detected in FG Vir. Applying equation (19) to FG Vir's frequency spectrum yields 10.4 close frequency pairs, which is slightly over half the number of observed close frequency pairs in this star. Also, as pointed out in Lenz et al. (2008), there are seven frequency pairs where the separation is below  $0.01 \text{ c d}^{-1}$ . Equation (19) would yield 1.12 very close frequency pairs for FG Vir. Furthermore, according to Breger & Pamyatnykh (2006a), close frequency pairs seem to cluster around radial modes, whereas a number of pairs in Fig. 7 are close to the mid-points between consecutive radial modes. Hence, an astrophysical origin is still needed to account for this phenomenon.

An interesting feature appears in Fig. 7. Between approximately  $0.02$  and  $0.05 \Omega_K$ , few frequency pairs are detected. A simple explanation is that the rotation rate is sufficient to keep individual multiplet components far enough apart, but too small to cause frequency multiplets to overlap. Of course, including modes with higher  $\ell$  values would probably reduce this gap by introducing new multiplets into the frequency spectrum. However, as was pointed out by Lignières et al. (2006); Lignières & Georgeot (2009), cancellation effects for such modes are more effective at lower rotation rates, i.e. where close frequency pairs are lacking. Table 2 gives a list of  $\delta$  Scuti stars where close frequencies have been reported. Interest-

**Table 2.** Projected equatorial velocities of  $\delta$  Scuti stars with observed close frequency pairs (this list is based on Breger & Bischof 2002; Lenz et al. 2008). The first two columns identify the star. The third and fourth columns give the projected equatorial velocity and the reference where this velocity is obtained.

Star	HD number	$v \cdot \sin i$ ( $\text{km s}^{-1}$ )	Reference
BI CMi	66853	$76 \pm 1$	Breger et al. (2002)
XX Pyx		$52 \pm 2$	Handler et al. (1997)
V509 Per	18878	134	Bush & Hintz (2008)
4 CVn	107904	$112 \pm 3^a$	Bush & Hintz (2008)
FG Vir	106384	$21.6 \pm 0.3^b$	Zima et al. (2006)
BV Cir	132209	$96.5 \pm 1$	Mantegazza et al. (2001)
BW Cnc	73798	$200 \pm 11$	Fossati et al. (2008)
44 Tau	26322	$2 \pm 1^c$	Zima et al. (2007)

<sup>a</sup> Bush & Hintz (2008) gave a list of several values. The value given here is the average plus or minus the standard deviation.

<sup>b</sup> Although the projected equatorial velocity is small, Zima et al. (2006) estimated that the true equatorial velocity is  $66 \pm 16 \text{ km s}^{-1}$ .

<sup>c</sup> Zima et al. (2007) estimated that the true equatorial velocity is  $3 \pm 2 \text{ km s}^{-1}$ .

ingly, none of the stars fall in this gap. Of course, a larger number of stars would need to be analysed to see whether this gap remains or whether it is simply due to poor statistics. Furthermore, some of the stars in Table 2, such as BI CMi (Breger et al. 2002), BV Cir (Mantegazza, Poretti & Zerbi 2001) and 44 Tau (Zima et al. 2007), are evolved. Consequently, their pulsation spectra are likely to contain acoustic, gravity (or gravito-inertial) and possibly mixed modes.

## 6 CONCLUSION

In this study, the effects of stellar rotation on acoustic pulsation frequencies have been investigated using a second-order perturbative and a two-dimensional approach. A comparison of the two shows that perturbative methods are valid for equatorial velocities of up to  $30$  and  $50 \text{ km s}^{-1}$  for a *CoRoT* long and short run, respectively. The associated validity domains closely match the domains previously obtained in Reese et al. (2006) for polytropic models. These results show that perturbative methods, which are simpler to work with and less demanding numerically, will remain useful for a number of stars. None the less, various qualitative and quantitative differences appear between this approach and two-dimensional calculations at sufficient rotation rates. Among these is the pairing up of adjacent modes in frequency multiplets. This phenomenon, first noted in Espinosa et al. (2004), also shows up in the two-dimensional calculations presented here but not in the second-order perturbative calculations, in which the spacing between consecutive modes varies monotonically. The cause of this pairing up remains a mystery, given that different modes in a multiplet are not coupled due to their differing azimuthal orders.

The case of observed close frequency pairs is then discussed. In particular, it is shown that adjacent mode pairs in frequency multiplets do not come close enough together to provide a likely explanation, as opposed to what was previously suggested (Espinosa et al. 2004). A systematic search for all of the close frequency pairs in the calculated spectra was then carried out. Results showed that at sufficient rotation rates, the number of close pairs of low degree acoustic modes matched what is expected based on a Poisson distribution. Even then, this does not match the number and distribution of close pairs observed in stars such as FG Vir, thereby favouring an astrophysical origin to the phenomena. At lower rotation rates, where frequency multiplets do not overlap, a lack of close frequency pairs is observed in the calculated spectra, except at the lowest rotation rates where the rotational shift is small.  $\delta$  Scuti stars currently reported as having close frequency pairs do not lie in this interval, but a more systematic study is required to see to what extent this is due to poor statistics. Furthermore, the effects of gravity type modes in more evolved stars need to be investigated.

## ACKNOWLEDGMENTS

The authors wish to thank the referee for useful comments which have helped to clarify the paper and improve the scientific discussion. DRR gratefully acknowledges support from the CNES ('Centre National d'Etudes Spatiales') through a post-doctoral fellowship, the UK Science and Technology Facilities Council through grant ST/F501796/1, and the European Helio- and Asteroseismology Network (HELAS), a major international collaboration funded by the European Commission's Sixth Framework Programme. This research has made use of the SIMBAD data base, operated at CDS, Strasbourg, France.

## REFERENCES

- Breger M., Bischof K. M., 2002, *A&A*, 385, 537  
 Breger M., Pamyatnykh A. A., 2006a, *MNRAS*, 368, 571  
 Breger M., Pamyatnykh A. A., 2006b, *Mem. Soc. Astron. Ital.*, 77, 295  
 Breger M. et al., 2002, *MNRAS*, 329, 531  
 Bush T. C., Hintz E. G., 2008, *AJ*, 136, 1061  
 Christensen-Dalsgaard J., 2008a, *Ap&SS*, 316, 13  
 Christensen-Dalsgaard J., 2008b, *Ap&SS*, 316, 113  
 Clement M. J., 1981, *ApJ*, 249, 746  
 Dziembowski W. A., Goode P. R., 1992, *ApJ*, 394, 670  
 Eggleton P. P., Faulkner J., Flannery B. P., 1973, *A&A*, 23, 325  
 Espinosa F., Pérez Hernández F., Roca Cortés T., 2004, in Danesy D., ed, *ESA SP Vol. 559, SOHO 14 Helio- and Asteroseismology: Towards a Golden Future Oscillation Modes in Axially Symmetric Stars*. ESA, Noordwijk, p. 424  
 Fossati L., Bagnulo S., Landstreet J., Wade G., Kochukhov O., Monier R., Weiss W., Gebran M., 2008, *A&A*, 483, 891  
 Gough D. O., Thompson M. J., 1990, *MNRAS*, 242, 25  
 Handler G. et al., 1997, *MNRAS*, 286, 303  
 Iglesias C. A., Rogers F. J., 1996, *ApJ*, 464, 943  
 Karami K., 2008, *Chin. J. Astron. Astrophys.*, 8, 285  
 Kjeldsen H., Christensen-Dalsgaard J., Handberg R., Brown T. M., Gilliland R. L., Borucki W. J., Koch D., 2010, *Astron. Nachr.*, 331, 966  
 Kurucz R. L., 1991, in *NATO ASIC Proc. Vol. 341, Stellar Atmospheres – Beyond Classical Models*. Reidel, Dordrecht, p. 441  
 Lenz P., Pamyatnykh A. A., Breger M., 2008, *J. Phys. Conf. Ser.*, 118, 012063  
 Lignières F., Geogot B., 2008, *Phys. Rev. E*, 78, 016215  
 Lignières F., Geogot B., 2009, *A&A*, 500, 1173  
 Lignières F., Rieutord M., Reese D., 2006, *A&A*, 455, 607  
 Lovekin C. C., Deupree R. G., 2008, *ApJ*, 679, 1499  
 MacGregor K. B., Jackson S., Skumanich A., Metcalfe T. S., 2007, *ApJ*, 663, 560  
 Mantegazza L., Poretti E., Zerbi F. M., 2001, *A&A*, 366, 547  
 Michel E. et al., 2008, *Communications Asteroseismology*, 156, 73  
 Ouazzani R.-M., Goupil M.-J., Dupret M.-A., Reese D., 2009, *Communications Asteroseismology*, 158, 283  
 Reese D., Lignières F., Rieutord M., 2006, *A&A*, 455, 621  
 Reese D. R., MacGregor K. B., Jackson S., Skumanich A., Metcalfe T. S., 2009, *A&A*, 506, 189  
 Saio H., 1981, *ApJ*, 244, 299  
 Soufi F., Goupil M.-J., Dziembowski W. A., 1998, *A&A*, 334, 911  
 Suárez J. C., Goupil M. J., Reese D. R., Samadi R., Lignières F., Rieutord M., Lochard J., 2010, *ApJ*, 721, 537  
 Yoshida S., Eriguchi Y., 2001, *MNRAS*, 322, 389  
 Zima W. et al., 2006, *A&A*, 455, 235  
 Zima W., Lehmann H., Stütz C., Ilyin I. V., Breger M., 2007, *A&A*, 471, 237

This paper has been typeset from a  $\text{\TeX}/\text{\LaTeX}$  file prepared by the author.